Supplementary Information (SI) for Journal of Materials Chemistry A.

Optimizing membrane structure through interfacial instability of two-component to increase mechanical and separation performance

Xin Zhong [a], *Zhiguang Guo* [a,b*]

[a] Ministry of Education Key Laboratory for the Green Preparation and Application of Functional Materials, Hubei University, Wuhan 430000, People's Republic of China.

[b] State Key Laboratory of Solid Lubrication, Lanzhou Institute of Chemical Physics, Chinese Academy of Sciences, Lanzhou 730000, People's Republic of China.

*Corresponding author. Tel: 0086-931-4968105; Fax: 0086-931-8277088. Email address: zguo@licp.cas.cn

Experimental Section

1 Materials

PVDF (average Mw ~ 400,000, powder, density: 1.78 g mL^{-1} at 25 °C) was purchased from Shanghai Macklin Biochemical Co., Ltd., China. PAN (average Mw ~ 149,000-151,000, density: 1.184 g mL^{-1} at 25 °C), PVP (average Mw ~ 10,000, K13-18, density: 1.144 g mL^{-1} at 25 °C) were purchased from Shanghai Aladdin Chemical Co., Ltd., China. N, N-Dimethylformamide (DMF, AR), Acetone (≥99.0%), SDS (CP) were purchased from Sinopharm Chemical Reagent Co., Ltd, Shanghai, China. CNT (inter diameter: 5-12 nm) was purchased from Shanghai Bidepharm Technology Co., Ltd., China. AMPS was purchased from Shanghai Xushuo Technology Co., Ltd., China. Deionized water was obtained from a water purifier (Ulupure-I-20T, Sichuan Ulupure Technology Co., Ltd.) with a resistivity of 18.25 MΩ cm. None of the reagents were further purified before use.

2 Preparation of Electrospun P-P-CNT-PVP Membrane

The fiber membranes were fabricated via electrospinning. The solvent of the spinning solution consisted of DMF and acetone in a ratio of 6:4. The polymer bicomponent was composed of PVDF and PAN, with a total mass of 16 wt% relative to the solvent and a mass ratio of 1:1, which was designated as P-P. On this basis, CNT were added at a concentration of 1 mg mL^{-1} in the total volume of the spinning solution, and dispersed uniformly by ultrasonication, resulting in the P-P-CNT. The P-P-CNT-PVP-n were prepared by additionally incorporating 1, 3, and 5 mg mL^{-1} of PVP into the spinning solution. All spinning precursors were stirred at 60 °C for 36 h to ensure complete dissolution of the polymers. Subsequently, the spinning precursors were loaded into a 10 mL syringe, and a high-voltage direct current of 11–13 kV was applied using a high-voltage power supply. The temperature was maintained at 32.5 ± 2.5 °C, and the relative humidity was kept at 35 ± 5%. The total spinning volume was 8 mL. The resulting fiber membranes were then placed in an oven at 95 ± 5 °C for 24 h to remove all solvents.

3 Material Characterization

The morphologies of samples were obtained via FESEM (sigma 500). The element distribution on the membrane surface was characterized by EDS (Bruker, XFlash 6/30). X-ray Photoelectron Spectroscopy (Thermo Scientific ESCALAB 250Xi) was hired to perform surface element composition analysis. The group types of the samples were characterized by FT-IR (is50). The crystal structures of the samples were determined via X-Ray Diffraction (Bruker, D8 Advance). Emulsion droplet sizes were measured by Particle Size and Z Potential Analyzer (Zetasizer Nano ZS90) and optical microscopy (Olympus). The fiber diameter was calculated using Nano Measure software. The JC2000D CA measuring instrument (Shanghai Zhongchen Digital Technology Equipment Co., Ltd.) was used to measure the sample's contact angle. The mechanical properties of the samples were tested using a high and low-temperature material testing machine (TM-10) and the modulus was calculated. The samples of each component were cut into a fixed size using a mold of 1 cm × 4 cm and their length, width, and thickness were measured using a vernier caliper.

4 Porosity and Pore Diameter Test

The samples were cut into a fixed size using a mold of 1 cm × 4 cm, with three replicates per group. The length, width, and thickness of each sample were precisely measured using a vernier caliper, and the samples were weighed. The apparent density (ρ) of the fiber membrane was calculated based on the measured mass and volume of each membrane. The porosity (ε) of the fiber membrane was calculated using Equation (1):

$$porosity\ (\%) = \frac{(\rho_0 - \rho)}{\rho_0} \times 100\%$$

Here, ρ_0 represents the density of the bicomponent raw material. Since the content of CNT and PVP is relatively low compared to PVDF and PAN, they are neglected in this calculation. ρ_0 is calculated using Equation (2):

$$\rho_0 = \frac{m_1 + m_2}{v_1 + v_2} = \frac{m_1 + m_2}{\frac{m_1}{\rho_1} + \frac{m_2}{\rho_2}}$$

Here, m_1, v_1, and ρ_1 represent the mass, volume, and density of the PVDF component, respectively. m_2, v_2, and ρ_2 represent the mass, volume, and density of the PAN component, respectively.

Pore diameter (*d*) of fiber membranes were calculated by using the Guerout-Elford-Ferry equation of filtration velocity method, as in Equation (3)[1,2]:

$$d = \sqrt{\frac{32 \times (2.9 - 1.75\varepsilon) \times J_W \times t \times \mu_W}{\varepsilon \times A \times P}}$$

Where, J_w is the water permeation flow rate. *t* is the membrane thickness. μ_w is the viscosity of water (8.9×10^{-4} Pa S). *A* is the effective area of the membrane. *P* is the operational pressure.

5 Pure Water Permeation Test and Emulsion Separation Test

The Pure Water Permeation performance of all membranes was evaluated using a dead-end filtration system with an effective area of 1.5 × 1.5 cm^2 under gravitational conditions. A 5-minute Pure Water Permeation flux test was performed. A minimum of three performances per sample were used to determine the average water flux value and expressed as the standard deviation of error. Flux (*J*) was calculated using the Equation (4):

$$J = \frac{V}{At}$$

Where, *V* is the volume of filtrate, and *t* is the recorded permeation time.

The emulsion separation experiment was conducted through a dead-end filtration method. The effective separation membrane area was 1.5 × 1.5 cm^2 under gravitational conditions. The emulsion separation performance of different components was investigated over a period of 5 min. The emulsion used in the experiment was prepared as follows: Toluene was used as the separation oil, and Tween 80 was employed as the surfactant. 100 mL of oil/water (2 v/v%) containing the surfactant (20 mg) was stirred at 6000 rpm for 0.5 h using a high-speed mixer (FJ-200-SH). The permeation flux was calculated using Equation (3), and the permeation efficiency was calculated using Equation (5):

$$R = \left(\frac{C_i - C_f}{C_i}\right) \times 100\%$$

where C_i is the concentration of oil in the emulsion before separation (g cm^{-1}) and C_f is the concentration of oil in the filtrate after separation (g cm^{-1}).

The continuous separation capability of the membrane was investigated by conducting 12 separation cycles with each cycle lasting 5 min. Additionally, a comparison was made between cycles with and without a cleaning process. The cleaning process involved rinsing the membrane with deionized water for 2 min between each separation cycle.

References

[1] M.N. Sarbolouki, Pore flow models and their applicability Ion Exch. Membr. 2(2) (1975) 117-122. https://doi.org/PMID: 1223013.

[2] D. Yadav, A. Karunanithi, S. Saxena, S. Shukla, Modified PVA membrane for separation of micro-emulsion, Sci. Total Environ. 822 (2022) 153610.

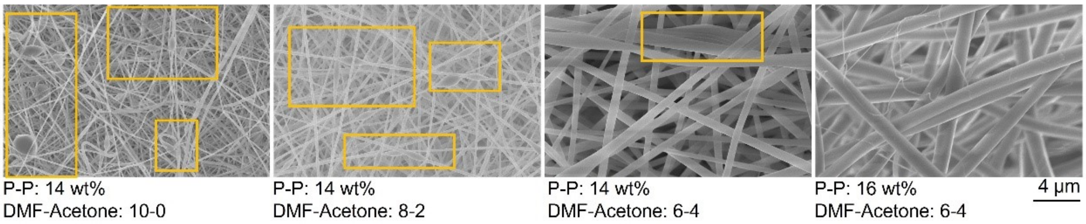

Fig. S1 SEM images of bicomponent composite membranes of PVDF and PAN with different component ratios and solvent compositions.

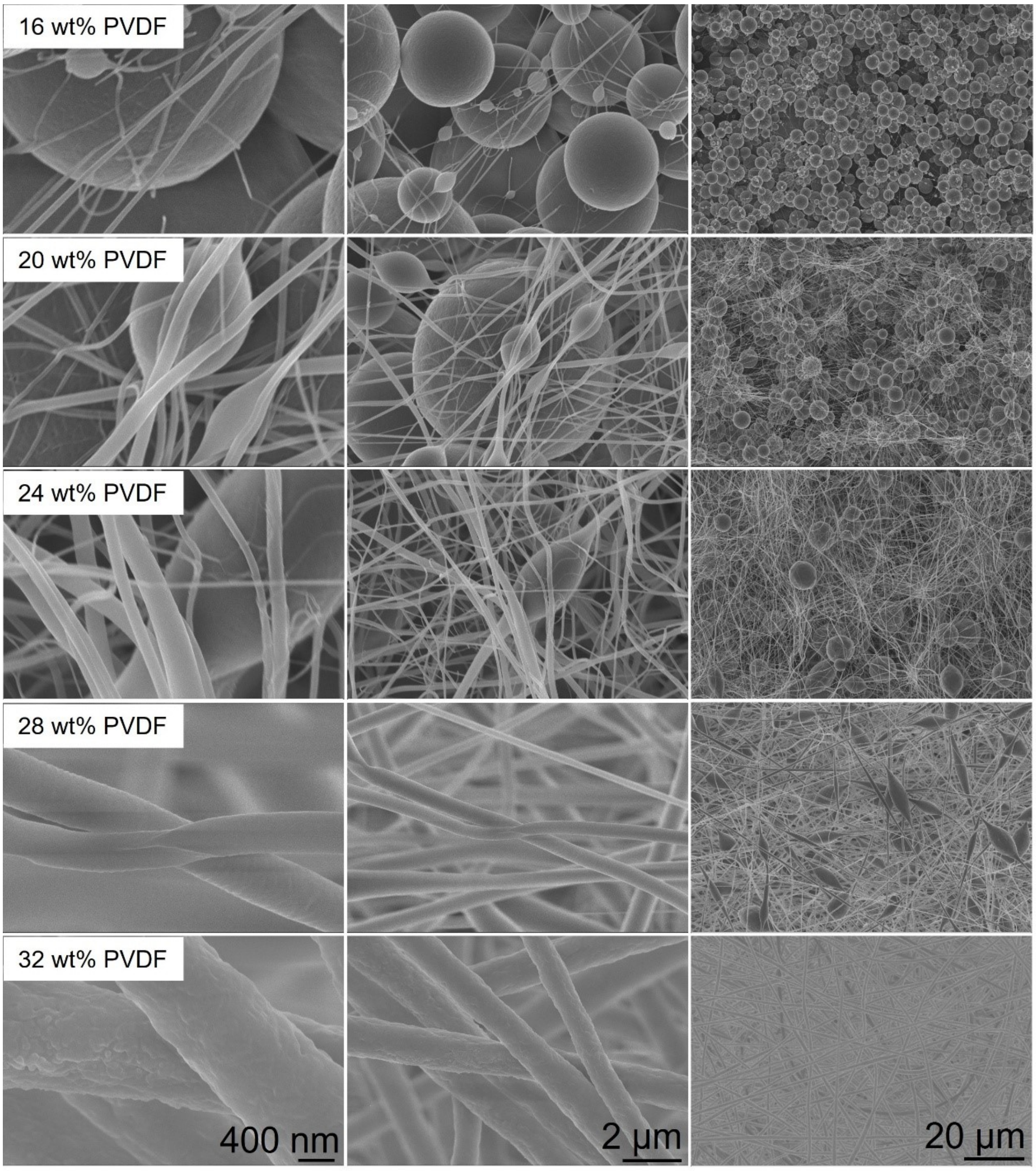

Fig. S2 SEM images of PVDF membranes prepared at different concentrations.

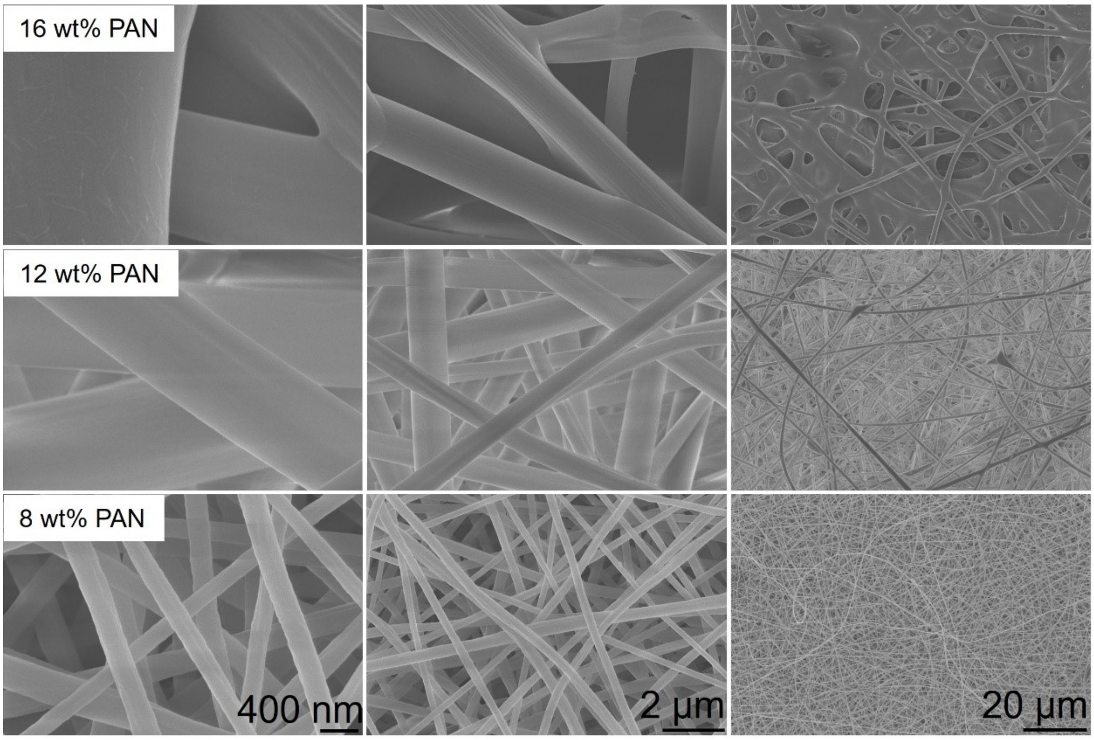

Fig. S3 SEM images of PAN membranes prepared at different concentrations.

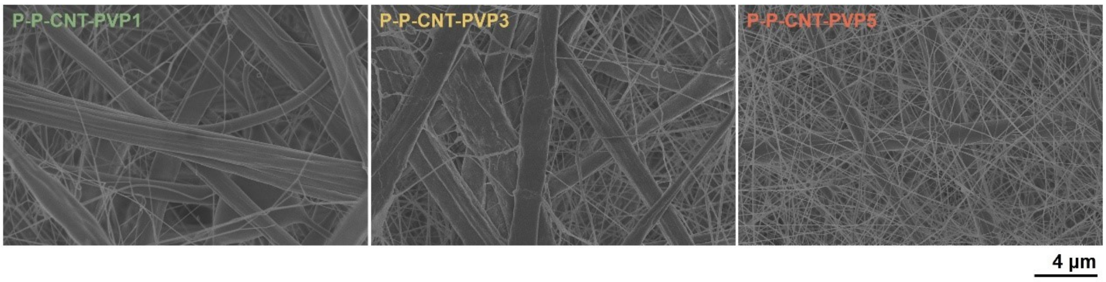

Fig. S4 SEM images of P-P-CNT-PVP-n membranes prepared at different PVP concentrations.

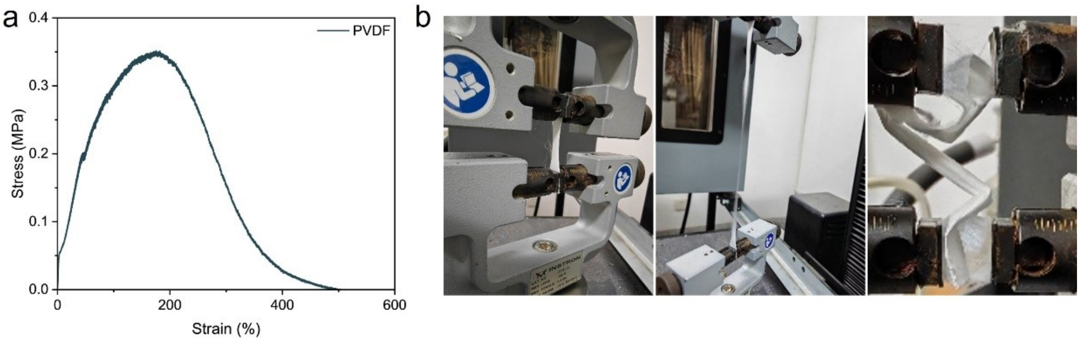

Fig. S5. (a) The mechanical tensile behavior of PVDF. (b) The adhesion phenomenon of PVDF when the clamp is removed.

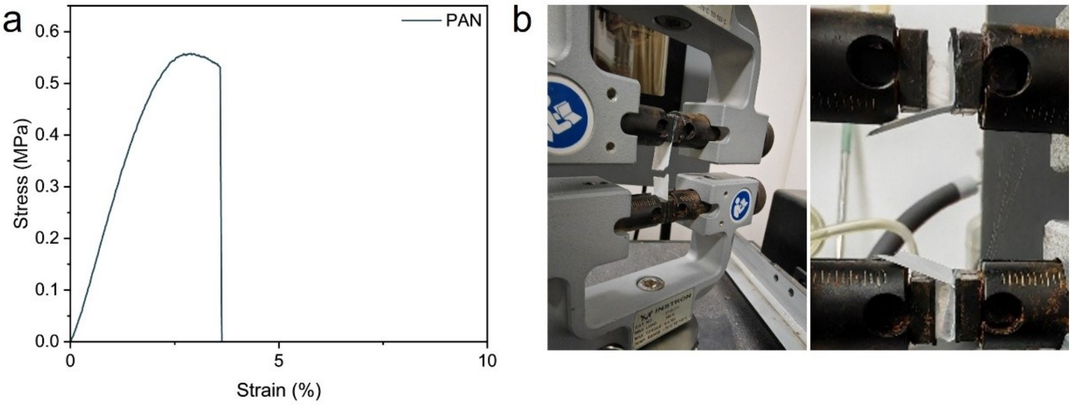

Fig. S6. (a) The mechanical tensile behavior of PAN. (b) The adhesion phenomenon of PAN when the clamp is removed.

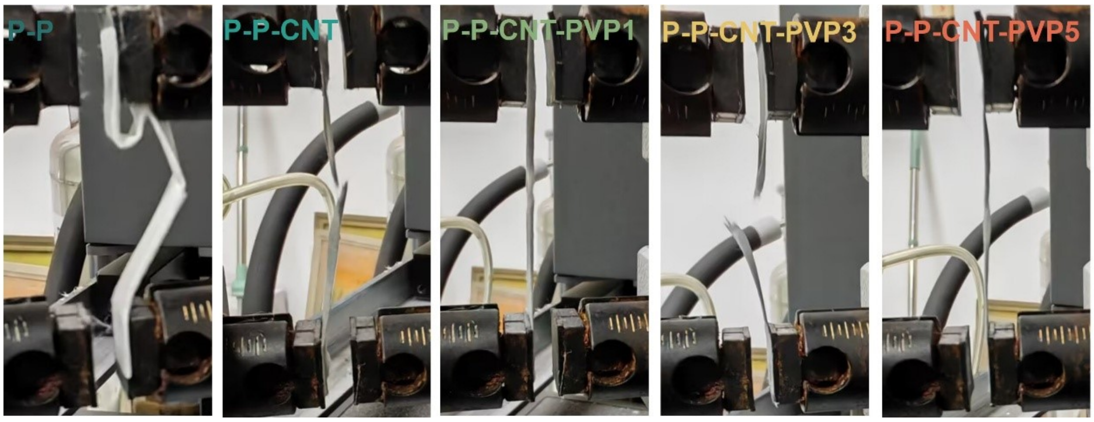

Fig. S7. Photos of the bicomponent fiber membrane after clamp detachment.

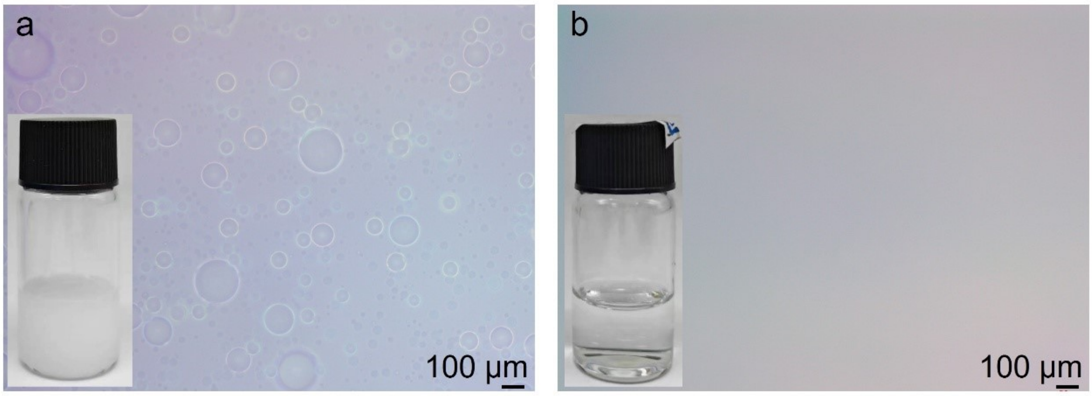

Fig. S8. Optical photographs of emulsions before (a) and after (b) separation.

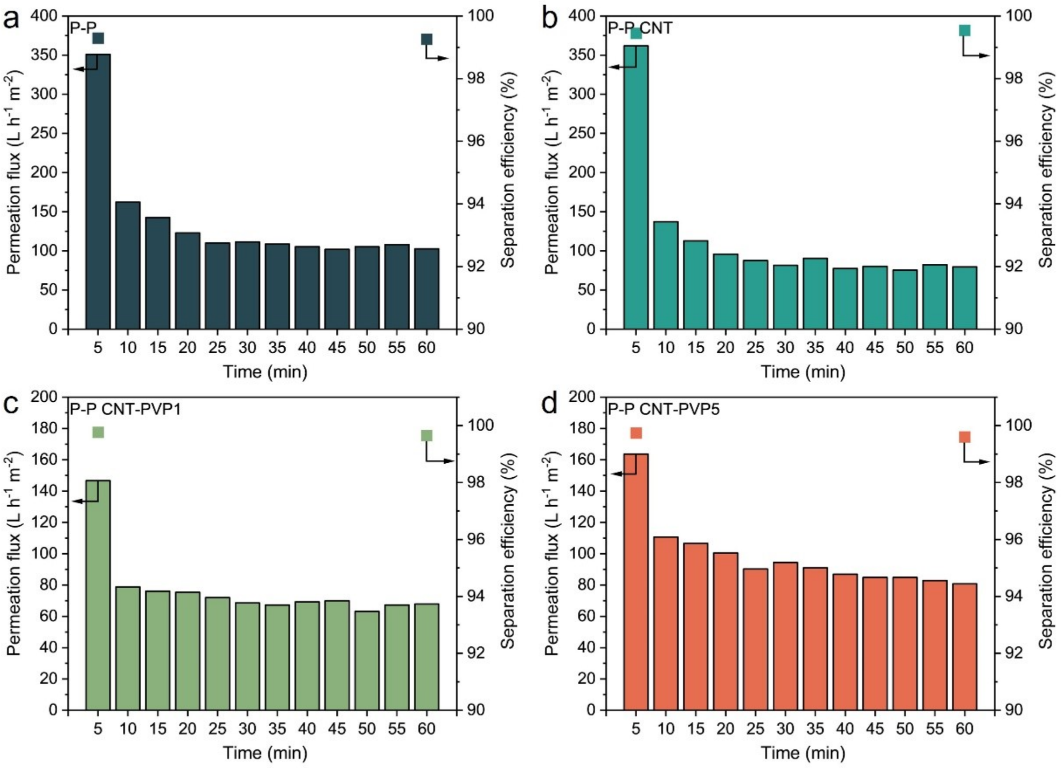

Fig. S9. Continuous emulsion separation diagram of P-P (a), P-P-CNT (b), P-P-CNT-PVP1 (c), and P-P-CNT-PVP5 (d) under uncleaned operation.